Simulation of Beam-Beam Effects and Tevatron Experience

A. Valishev,* Yu. Alexahin, and V. Lebedev

Fermilab, Batavia, IL 60510, USA

D. Shatilov

BINP SB RAS, Novosibirsk, 630090, Russia

(Dated: June 1, 2009)

Abstract

Effects of electromagnetic interactions of colliding bunches in the Tevatron have a variety of manifestations in beam dynamics presenting vast opportunities for development of simulation models and tools. In this paper the computer code for simulation of weak-strong beam-beam effects in hadron colliders is described. We report the recent operational experience, explain major effects limiting the collider performance and compare results of observations and measurements with simulations.

PACS numbers: 29.27.Bd

*Electronic address: valishev@fnal.gov

I. INTRODUCTION

Peak luminosity of the Tevatron reached 3.5×10^{32} cm^{-2}s^{-1} which exceeds the original Run II goal of 2.7×10^{32}. This achievement became possible due to numerous upgrades in the antiproton source, injector chain, and in the Tevatron collider itself. The most notable rise of luminosity came from the commissioning of electron cooling in the recycler ring and advances in the antiproton accumulation rate. Starting from 2007, the intensity and brightness of antiprotons delivered to the collider greatly enhanced the importance of beam-beam effects. Several configurational and operational improvements in the Tevatron have been planned and implemented in order to alleviate these effects and allow stable running at high peak luminosities.

Since the publication of paper [1] that gave a detailed summary of beam dynamics issues related to beam-beam effects, the peak luminosity of Tevatron experienced almost a tree-fold increase. In the present article we provide an updated view based on the recent years operation (Section II).

Development of a comprehensive computer simulation of beam-beam effects in the Tevatron started in 1999. This simulation proved to be a useful tool for understanding existing limitations and finding ways to mitigate them. In Section IV the main features of the code LIFETRAC are described. In Sections V-VI we summarize our experience with simulations of beam-beam effects in the Tevatron, and cross-check the simulation results against various experimental data and analytical models. We also correlate the most notable changes in the machine performance to changes of configuration and beam conditions, and support the explanations with simulations.

II. OVERVIEW OF BEAM-BEAM EFFECTS

A detailed description of the Tevatron collider Run II is available in other sources [2]. Here only the essential features important for understanding of beam dynamics are provided.

Tevatron is a superconducting proton-antiproton collider ring in which beams of the two species collide at the center of mass energy of 2×0.98 TeV at two experiments. Each beam consists of 36 bunches grouped in 3 trains of 12 with 396 ns bunch spacing and 2.6 μs abort gaps between the trains. The beams share a common vacuum chamber with both

beams moving along helical trajectories formed by electrostatic separators. Before the high energy physics collisions have been initiated, the proton and antiproton beams can be moved longitudinally with respect to each other, which is referred to as cogging. This configuration allows for 72 interactions per bunch each turn with the total number of collision points in the ring equal to 138. The total number of collision points is determined by the symmetry of bunch filling pattern.

At the peak performance Tevatron operates with $N_p = 2.8{\cdot}10^{11}$ protons and $N_a = 0.9{\cdot}10^{11}$ antiprotons per bunch. The normalized transverse 95% beam emittances are $\varepsilon_p = 18 \cdot 10^{-6}$m for protons and $\varepsilon_a = 7 \cdot 10^{-6}$m for antiprotons. Proton and antiproton bunch length at the beginning of a high energy physics (HEP) store is 52 cm and 48 cm, respectively. Parameters of the beams are mostly determined by the upstream machines.

The value of β-function at the main collision points (β^*) is 0.28 m. Betatron tunes are $Q_x = 20.584$, $Q_y = 20.587$ for protons and $Q_x = 20.575$, $Q_y = 20.569$ for antiprotons.

A typical collider fill cycle is shown in Figure 1. First, proton bunches are injected one at a time on the central orbit. After that, the helix is opened and antiproton bunches are injected in batches of four. This process is accompanied by longitudinal cogging after each 3 transfers. Then the beams are accelerated to the top energy (85 s) and the machine optics is changed to collision configuration in 25 steps over 120 seconds (low-beta squeeze). The last two stages include initiating collisions at the two main interaction points (IP) and removing halo by moving in the collimators.

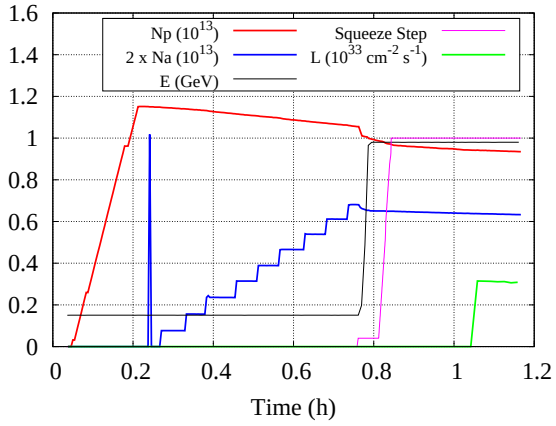

FIG. 1: Collider fill cycle for store 5989.

It has been shown in machine studies that beam losses up the ramp and through the

low-beta squeeze are mainly caused by beam-beam effects [1]. In the HEP mode, the beam-beam induced emittance growth and particle losses contribute to the faster luminosity decay. Figure 2 summarizes the observed losses of luminosity during different stages of the collider cycle.

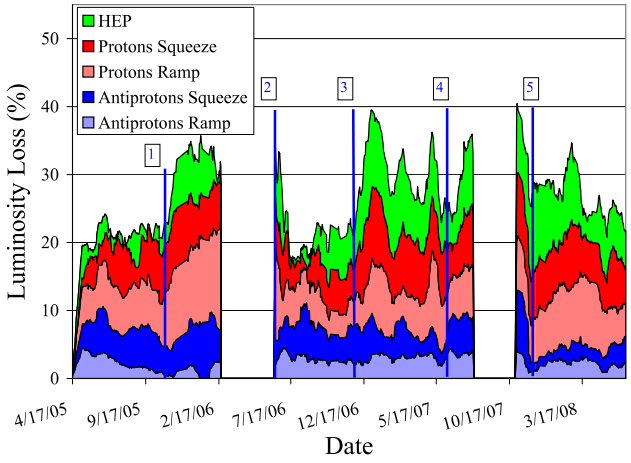

FIG. 2: Luminosity loss budget over a 3 year period. The labels mark: 1. Commissioning of electron cooling. 2. Installation of extra separators and new collision helix. 3. Antiproton accumulation rate. 4. Correction of second-order chromaticity. 5. Implementation of antiproton emittance blowup.

A. Beam-beam effects at injection

During injection the long range (also referred to as parasitic) beam-beam effects cause proton losses (currently 5 to 10%). At the same time the antiproton life time is very good and only a fraction of a per cent are lost. Observations show that mainly off momentum particles are lost (Fig. 3) and the betatron tune chromaticity $C = dQ/d\delta$, where $\delta = \Delta p/p$ is the relative momentum deviation, has a remarkable effect. Early in Run II the chromaticity had to be kept higher than 8 units in order to maintain coherent stability of the intense proton beam, but after several improvements aimed at reduction of the machine impedance the chromaticity is about 3 units [3, 4, 5]. Figure 3 shows an interesting feature in the behavior of two adjacent proton bunches (no. 20 and 21). Spikes in the measured values are instrumental effects labeling the time when the beams are cogged. Before the first cogging the bunches have approximately equal life time. After the first cogging bunch 20

exhibits faster decay, and bunch 21 after the second. Analysis of the collision patterns for these bunches allowed to pinpoint a particular collision point responsible for the life time degradation. The new injection helix has been implemented late in 2007 which improved the proton life time [6, 7].

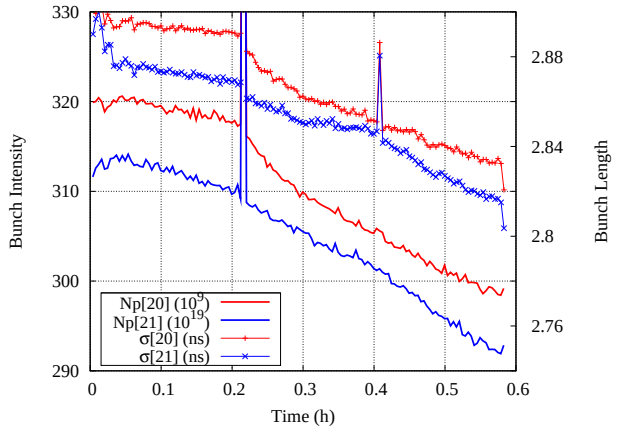

FIG. 3: Intensity and length of proton bunches no. 20 and 21 during injection of antiprotons.

B. Low-beta squeeze

During the low-beta squeeze two significant changes occur - the β^* value is being gradually decreased from $\sim$1.5 m to 0.28 m (hence the name squeeze) and the helical orbits change their shape and polarity from injection to collision configuration. The latter poses a serious limitation since the beams separation at several long range collision points briefly decreases from 5-6σ to $\sim 2\sigma$. At this moment a sharp spike in losses is observed.

Another important operational concern was the tight aperture limitation in one of the two final focus regions (CDF). With dynamically changing orbit and lattice parameters the local losses were often high enough to cause a quench of the superconducting magnets even though the total amount of beam loss is small ($\sim$ 1%). The aperture restriction has been located and fixed in October of 2008.

Besides orbit stability two other factors were found to be important in maintaining low losses through the squeeze: antiproton beam brightness and betatron coupling. Figure 4 shows the dependence of proton losses on the antiproton beam brightness. Large amount of stores lost in this stage of the cycle caused by increase of the antiproton beam brightness

after the 2007 shutdown demanded the commissioning of the antiproton emittance control system [8].

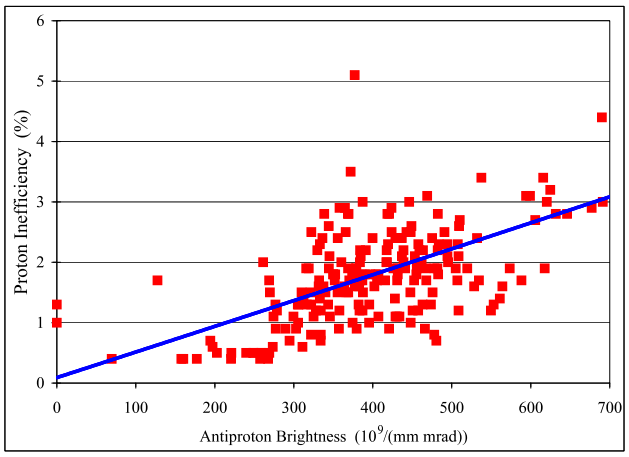

FIG. 4: Proton losses in low-beta squeeze vs. antiproton beam brighness $36 \cdot N_a/\varepsilon_a$.

C. High energy physics

After the beams are brought into collisions at the main IPs, there are two head-on and 70 long range collision points per bunch. Beam-beam effects caused by these interactions lead to emittance growth and particle losses in both beams.

During the running prior to the 2006 shutdown the beam-beam effects at HEP mostly affected antiprotons. The long range collision points nearest to the main IPs were determined to be the leading cause for poor life time. Additional electrostatic separators were installed in order to increase the separation at these IPs from 5.4 to 6σ [7]. Also, the betatron tune chromaticity was decreased from 20 to 10 units. Since then, the antiproton life time is dominated by losses due to luminosity and no emittance growth is observed provided that the betatron tune working point is well controlled.

Electron cooling of antiprotons in the Recycler and increased antiproton staching rate drastically changed the situation for protons. Figure 5 shows the evolution of total head-on beam-beam tune shift ξ for protons and antiprotons. Note that prior to the 2006 shutdown the proton ξ was well under 0.01 and big boost occurred in 2007 when both beam-beam parameters became essentially equal. It was then when beam-beam related losses and emittance blowup started to be observed in protons.

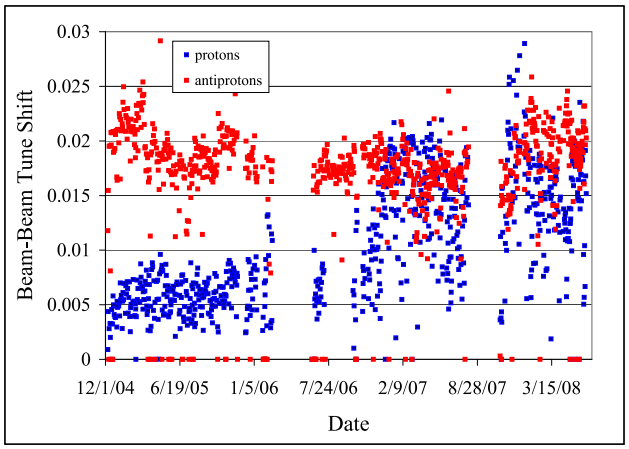

FIG. 5: Head-on beam-beam tune shift vs. time.

Our analysis showed that deterioration of the proton life time was caused by a decrease of the dynamical aperture for off-momentum particles due to head-on collisions (see Sec. VI). It was discovered that the Tevatron optics had large chromatic perturbations, e.g. the value of β^* for off-momentum particles could differ from that of the reference particle by as much as 20%. Also, the high value of second order betatron tune chromaticity $d^2Q/d\delta^2$ generated a tune spread of $\sim$0.002. A rearrangement of sextupoles in order to correct the second order chromaticity was planned and implemented before the 2007 shutdown [9]. Figure 6 demonstrates the effect of this modification on integrated luminosity. Since the dependence of luminosity on time is very well fitted by a $L_0/(1 + t/\tau)$ function, one can normalize the luminosity integral for a given store to a fixed length T_0 by using the expression $L_0\tau \cdot ln(1 + T_0/\tau)$ [10]. Here L_0 is the initial luminosity, and τ is the luminosity life time. One can see that after the modification the saturation at luminosities above 2.6×10^{32} was mitigated and the average luminosity delivered to experiments increased by $\sim$ 10%.

Another step in the proton ξ happened after the 2007 shutdown when the transverse antiproton emittance decreased because of improvements in injection matching. The total attained head-on beam-beam tune shift for protons exceeded that of antiprotons and reached 0.028. This led to high sensitivity of the proton life time to small variations of the betatron tunes, and to severe background conditions for the experiments. The reason is believed to be the large betatron tune spread generated by collisions of largely different size bunches [11]. Indeed, at times the antiproton emittance was a factor of 5 to 6 smaller than the proton emittance.

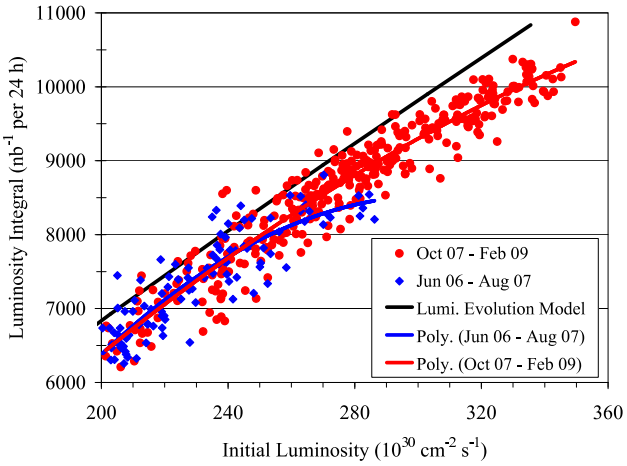

FIG. 6: Luminosity integral normalized by 24 h vs. initial luminosity. Blue points and curve - before second order chromaticity correction, red - after correction. Black line represents the ultimate integral for the given beam parameters in the absence of beam-beam effects (see Sec. III).

To decrease the proton to antiproton emittance ratio a system has been commissioned which increases the antiproton emittance after the top energy is reached by applying wide band noise to a directional strip line (line 5 in Fig. 2) [8]. Currently, the optimal emittance ratio is $\sim$3.

Since the majority of our efforts was targeting beam-beam effects in HEP mode, we concentrate on this topic in the remaining part of this paper. Discussion of long range effects at injection and coherent effects [12] is left out of the scope of this report.

III. STORE ANALYSIS PACKAGE

Beam-beam interaction is not the single strongest effect determining evolution of beam parameters at collisions. There are many sources of diffusion causing emittance growth and particle losses, including but not limited to intrabeam scattering, noise of accelerating RF voltage, and scattering on residual gas. Parameters of these mechanisms were measured in beam studies, and then a model was built in which the equations of diffusion and other processes are solved numerically [13]. This model is able to predict evolution of the beam parameters in the case of weak beam-beam effects. When these effects are not small, it provides a reference for evaluation of their strength. We use this approach on a store-by-store basis to monitor the machine performance in real time [14] because such calculations

are very fast compared to a full numerical beam-beam simulation. Figure 7 presents an example comparison of evolution of beam parameters in an actual high luminosity store to calculations. Note that there is no transverse emittance blow up in both beams, and the emittance growth is determined by processes other than beam-beam interaction. The same is true for antiproton intensity and bunch length. The most pronounced difference between the observation and the model is seen in the proton intensity. Beam-beam effects cause proton life time degradation during the initial 2-3 hours of the store until the proton beam-beam tune shift drops from 0.02 to 0.015. The corresponding loss of luminosity integral is about 5%.

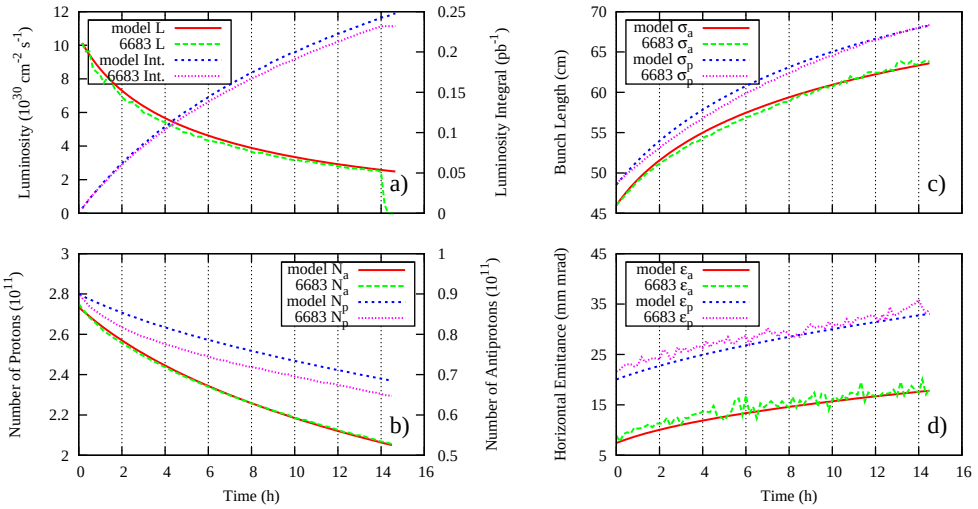

FIG. 7: Observed beam parameters in store 6683 compared to store analysis calculation (model). $L_0 = 3.5 \cdot 10^{32}$ cm^{-2} s^{-1}. a) Single bunch Luminosity and Luminosity integral. b) Intensity of proton bunch no. 6 and of antiproton bunch colliding with it (no. 13). c) Bunch lengths. d) Horizontal 95% normalized bunch emittances.

IV. WEAK-STRONG CODE LIFETRAC

Initially, the beam-beam code LIFETRAC was developed for simulation of the equilibrium distribution of the particles in circular electron-positron colliders [15]. In 1999 the new features have been implemented, which allowed simulating non-equilibrium distributions, for example proton beams. In this case the goal of simulations is not to obtain the equilibrium distribution but to observe how the initial distribution is changing with time. Number of

simulated particles can vary in the range of 10^3 to 10^6, usually it is set to $(5 \div 10) \cdot 10^3$. The tracking time is divided into "steps", typically $10^3 \div 10^5$ turns each. The statistics obtained during the tracking (1D histograms, 2D density in the space of normalized betatron amplitudes, luminosity, beam sizes and emittances) is averaged over all particles and all turns for each step. Thus, a sequence of frames representing evolution of the initial distribution is obtained.

Another important quantity characterizing the beam dynamics is the intensity life time. It is calculated by placing an aperture restriction in the machine and counting particles reaching the limit. The initial and final coordinates of the lost particle are saved. This information is valuable for analysis of various beam dynamics features.

The initial 6D distribution of macroparticles can be either Gaussian (by default), or read from a separate text file. Besides, the macroparticles may have different "weights". This allows representing the beam tails more reliably with limited number of particles. Usually we simulate the Gaussian distribution with weights: particles initially located in the core region have larger weight while the "tail" particles with smaller weight are more numerous.

In the present bunch pattern (3 trains of 12 bunches) there are two main IPs and 70 long range collision points. When performing transformation through a main IP, the "strong" bunch is divided into slices longitudinally. The higher are the orders of significant betatron resonances which are supposed to make effect on the distribution, the greater must be the number of slices. In our simulations 12 slices were used in the main IPs where beta-functions are approximately equal to the bunch length and only one slice in long range collision points where beta-functions are much greater and one can neglect the betatron phase advance on the bunch length.

The transverse density distributions within "strong" slices are bi-Gaussian, allowing to apply the well-known formulae [16] for 6D symplectic beam-beam kick. However, a simple modification allowed simulating non-Gaussian strong bunches. Namely, the strong bunch is represented as a superposition of a few (up to three) Gaussian distributions with different betatron emittances. The kicks from all these "harmonics" are summarized additively. The calculation time is increased somehow (not very significantly) but the transformation remains 6D symplectic.

A. Tevatron optics

The parasitic collisions in Tevatron play a significant role in the beam dynamics. In order to account their contribution correctly an accurate knowledge of the machine lattice of the whole ring with all distortions, beta beatings, coupling, etc. is required. This necessitated the construction of a realistic model of the machine lattice based on beam measurements. The most effective method proved to be the orbit responce matrix analysis [17, 18, 19].

The model lattice is built in the optics code OptiM [20]. Both OptiM and LIFETRAC treat betatron coupling using the same coupled beta-functions formalism [21]. This allows the linear transport matrix between any two points to be easily derived from the coupled lattice functions and phase advances.

A set of scripts has been created enabling fast creation of input files for the beam-beam simulation. These programs automate calculation of azimuthal positions of interaction points for the chosen bunch and extraction of the optics parameters. In the end, the machine optics is represented by a set of 6D linear maps between the interaction points.

It was estimated that resonances generated by known Tevatron nonlinearities, such as the final focus triplets and lattice sextupoles, are much weaker than those driven by beam-beam collisions at the present betatron tune working point. Hence, inclusion of nonlinear lattice elements into the simulation was deemed unnecessary.

B. Chromaticity

Although linear optics is used for the machine lattice model, there are two nonlinear lattice effects which are considered to be significant for beam-beam behaviour and were included into simulations. These are the chromaticities of beta-functions excited in the Main IPs and chromaticities of the betatron tunes. In the Hamiltonian theory the chromaticity of beta-functions does not come from energy-dependent focusing strength of quads (as one would intuitively expect) but from drift spaces where the transverse momentum is large (low-beta regions). The symplectic transformations for that are:

$$X = X - L \cdot X' \cdot \frac{\Delta p}{p}$$
$$Y = Y - L \cdot Y' \cdot \frac{\Delta p}{p}$$

$$Z \;=\; Z - L \cdot (X'^2 + Y'^2)/2$$

where X, Y, and Z are the particle coordinates, and L is the "chromatic drift" length. Then, it is necessary to adjust the betatron tune chromaticities which are also affected by "chromatic drift". For that, an artificial element (insertion) is used with the following Hamiltonian:

$$H = I_x \cdot (2\pi Q_x + C_x \frac{\Delta p}{p}) + I_y \cdot (2\pi Q_y + C_y \frac{\Delta p}{p}),$$

where I_x and I_y are the action variables, Q_x and Q_y are the betatron tunes, C_x and C_y are the [additions to the] chromaticities of betatron tunes.

C. Diffusion and Noise

Diffusion and noise are simulated by a single random kick applied to the macroparticles once per turn. Strength of the kick on different coordinates is given by a symmetrical matrix representing correlations between Gaussian noises. In the Tevatron, the diffusion is rather slow in terms of the computer simulation – the characteristic time for the emittance change is around an hour, or $\sim 10^8$ turns. In order to match the diffusion and the computer capabilities, the noise was artificially increased by three orders of magnitude.

We justify this approach below. In contrast to the electron-positron colliders there is no damping in hadron colliders. As the result, during the store time an effect of beam-beam interaction on the emittance growth needs to be minimized and made small relative to other diffusion mechanisms such as the intra-beam scattering (IBS), scattering on the residual gas, and diffusion due to RF phase noise. We will call these the extrinsic diffusion to distinguish from the diffusion excited by beam-beam effects. For the present Tevatron parameters the extrinsic diffusion sets the luminosity lifetime to be about 10 hours at the beginning of the store. IBS dominates both transverse and longitudinal diffusions in the case of protons while its relative effect is significantly smaller for antiprotons because of $\sim$5 times smaller intensity.

Table I summarizes lifetimes for major beam parameters obtained with diffusion model [22] for a typical Tevatron store with the luminosity of $9 \times 10^{31} cm^{-2} s^{-1}$. There are many parameters in Tevatron which are beyond our control and therefore each store is different. For good stores, the beam-beam effects make comparatively small contribution to the emittance growth yielding luminosity lifetime in the range of 7-8 hours and 10-15% loss in the

luminosity integral. The planned threefold increase in antiproton intensity will amplify the beam-beam effects. That, if not addressed, can cause unacceptably large background in detectors and reduce integrated luminosity. In this paper we discuss the results of numerical simulations aimed to understand major factors contributing to the beam-beam interaction and possible ways of their mitigation.

Parameter (lifetime, hour)	**Protons**	**Antiprotons**
Luminosity	9.6	9.6
Transverse emittance, $(d\epsilon/dt)/\epsilon$ [hor./vert.]	-17 / -18	-52 / -46
Longitudinal emittance	-8	-26
Intensity	26	155

TABLE I: Lifetimes for major beam parameters obtained with diffusion model.

Under the real conditions at Tevatron the emittance growth rate is small and exact simulations of beam-beam effects would require tracking for billions of turns. That is well beyond capabilities of present computers. Fortunately, the extrinsic diffusion is large enough in comparison with beam-beam diffusion which resuls in the loss of phase correlation after about 50,000 turns.

The external noise plays important role in particle dynamics: it provides particle transport in the regions of phase space which are free from resonance islands.

To make this transport faster we can artificially increase the noise level assuming that its effect scales as noise power multiplied by number of turns. If we choose it so that the noise alone gives 10% emittance growth in 10^6 turns (we use this level as the reference) then this number of turns of simulation will correspond to ~ 5 h of time in the Tevatron.

To verify this approach we studied the effect of the noise level on luminosity using reconstructed optics.

Fig.8 presents results of the tune scan along the main diagonal with the reference noise level and without noise. The effect of noise on luminosity corresponds to its level with exception for the point $Q_y = 0.575$ where it was larger due to some cooperation with strong 5th order resonances.

To study this cooperation in more detail we performed tracking at this working point with different noise levels. Fig.9 shows the luminosity reduction in $2 \cdot 10^6$ turns (diamonds)

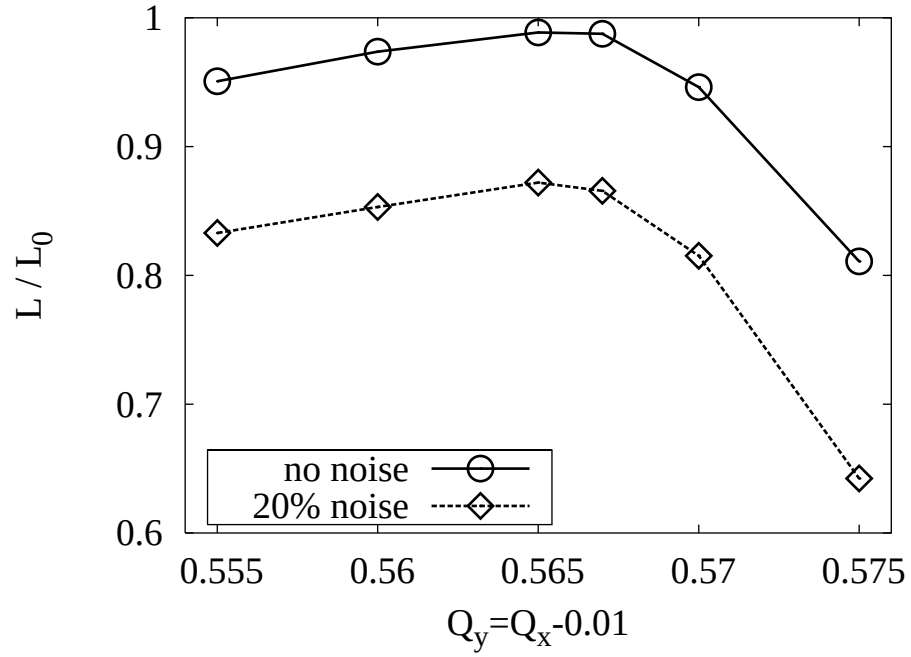

FIG. 8: Ratio of luminosity after a fixed time ($t = 2 \cdot 10^6$ turns) to the initial luminosity vs. betatron tune. Circles - $D_{noise} = 0$, diamonds - the emittance change due to extrinsic diffusion after t is 20%.

and a fit made using just 3 points, with relative noise level 0.5, 1 and 2.

The fit works fine for higher noise level, but predicts somewhat faster luminosity decay in absence of noise than actually observed in tracking. This means that there are regions in the phase space which particles cannot pass (within the tracking time) without assistance from the external noise so that the simple rule $D_{total} = D_{res} + D_{noise}$ does not apply. However, such "blank spaces" may contain isolated resonance islands which would show up on a longer time scale with the real level of external noise. The applicablity of this rule at the reference noise level testifies that (with the chosen number of turns) no such "blank spaces" were left so we get more reliable predictions.

D. Program features

Since the beam-beam code uses the "weak-strong" model, it can be very efficiently parallelized. Each processor tracks its own set of particles and the nodes need to communicate very rarely (at the end of each step), just to gather the obtained statistics. Hence, the

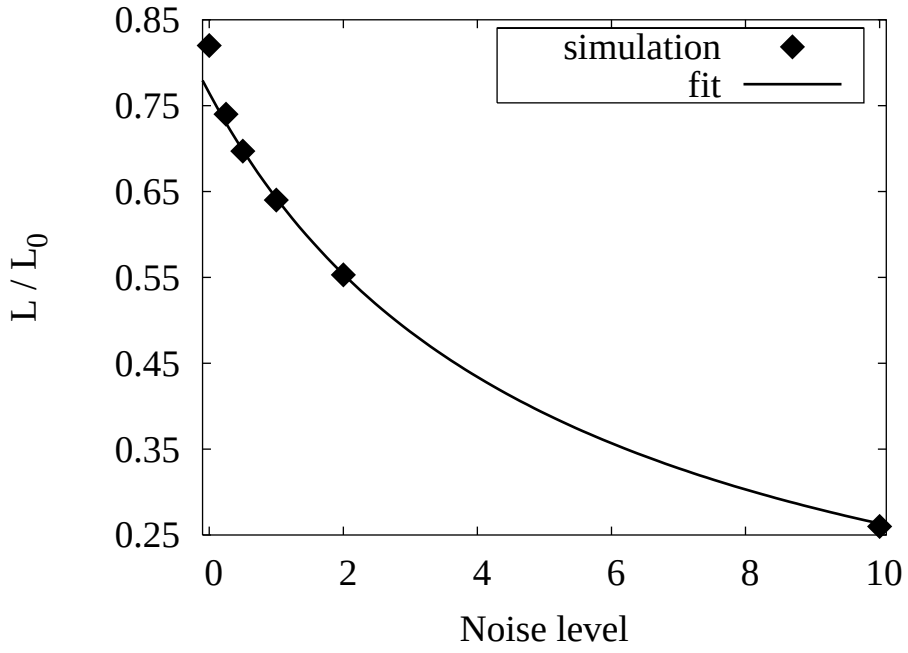

FIG. 9: Ratio of luminosities vs. noise level.

productivity grows almost linearly with the number of nodes.

There are also two auxiliary GUI codes. The first one automates production of the LIFETRAC input files for different bunches from the OptiM machine lattice files. The second one is dedicated for browsing the LIFETRAC output files and presenting the simulation results in a text and graphical (histogram) form.

We have validated the code using available experimental data. As an example, Figs. 10 and 11 show a good reproduction of the two distinct effects in bunch to bunch differences caused by beam-beam effects: variation of vertical bunch centroid position due to long range dipole kicks, and variation of transverse emittance blowup caused by difference in tunes and chromaticities.

The numerical simulation was used to justify the decrease of antiproton betatron tune chromaticity, reduction of the β^* from 0.35 m to 0.28 m (both in 2005). Importance of separation at the long range collision points nearest to the main IPs was also demonstrated.

Planning for the increase in amount of antiprotons available to the collider, we identified the large chromaticity of β^* as a possible source of the proton life time deterioration. Figure 12 shows the beam-beam induced proton life time for different values of ξ, and demonstrates the positive effect of corrected chromatic β^*.

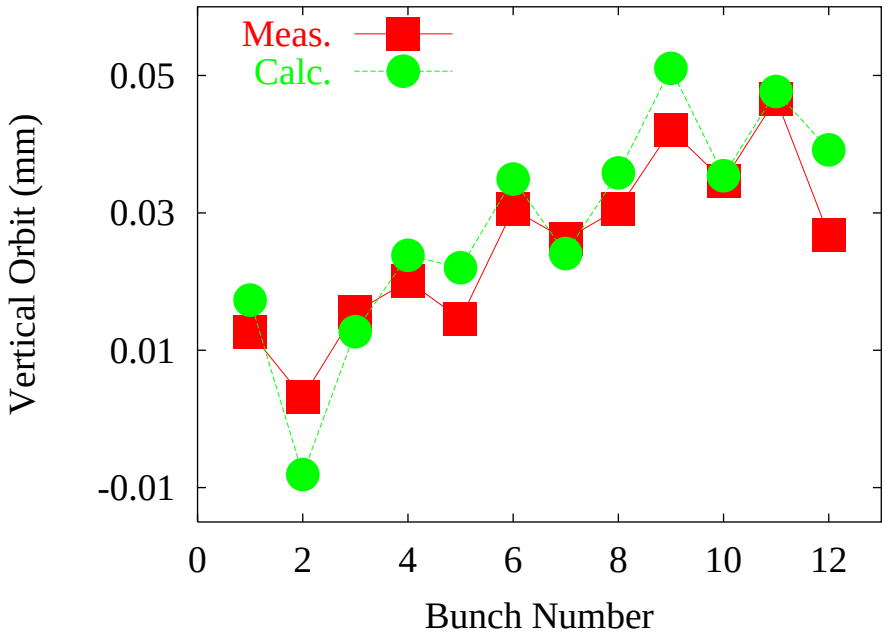

FIG. 10: Bunch by bunch antiproton vertical orbit.

Simulations revealed an interesting feature in the behavior of the proton bunch length at high values of ξ - the so-called bunch shaving, when the bunch length starts to decrease after initiating head-on collisions instead of steady growth predicted by the diffusion model (Fig. 13). This behavior was observed multiple times during HEP stores in 2007, being especially pronounced when the vertical proton betatron tune was set too high.

The significance of the PCs is illustrated in Fig. 14, where a bunch intensity is plotted vs. time (2×10^6 turns correspond to about 15 hours in the Tevatron) with the complete set of IPs and PCs, and with PCs turned off. It is clear that PCs dominate the particle losses.

E. Optics Errors

In the simulations we used 3 major Tevatron optics modifications:

- "design" optics with ideal parameters of the main Interaction Points (IP), zero coupling.
- "january" optics which was in effect until March, 2004. This optics was measured in January, 2004, and had sufficient distortions in the main IPs (unequal beta's, beam waists shifted from the IP), and betatron coupling.

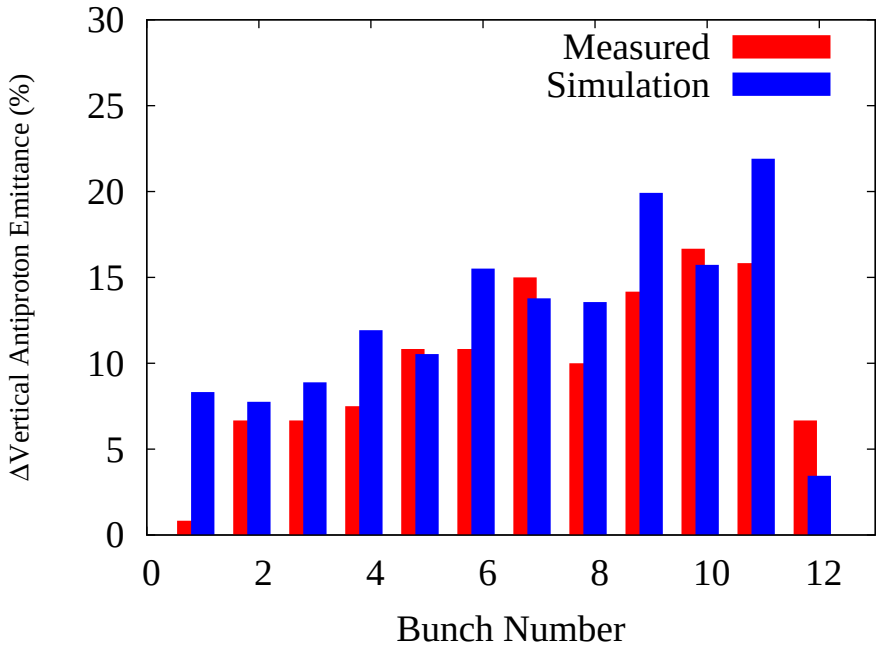

FIG. 11: Bunch by bunch antiproton emittance growth. Measured in store 3554 (red) and simulated with lifetrac (blue).

- "june" optics introduced in March, 2004, where the distortions were corrected.

Comparison of the three cases is shown in Fig. 15. This plot shows that modifications to the optics implemented in March, 2004, made the optics close to the design. Additional simulations revealed that the main source of particle losses was in the long range collisions (PC) nearest to the main IPs. Increasing the beams separation in these points and repairing the phase advances cured high antiproton losses.

F. Scallops

Another illustration of validity of the code is simulation of scallops. Fig. 11 shows the simulated pattern of the antiproton emittance blow-up during first minute of the store. We also demonstrated that scallops can be reduced by moving the working point farther from 5th order resonance.

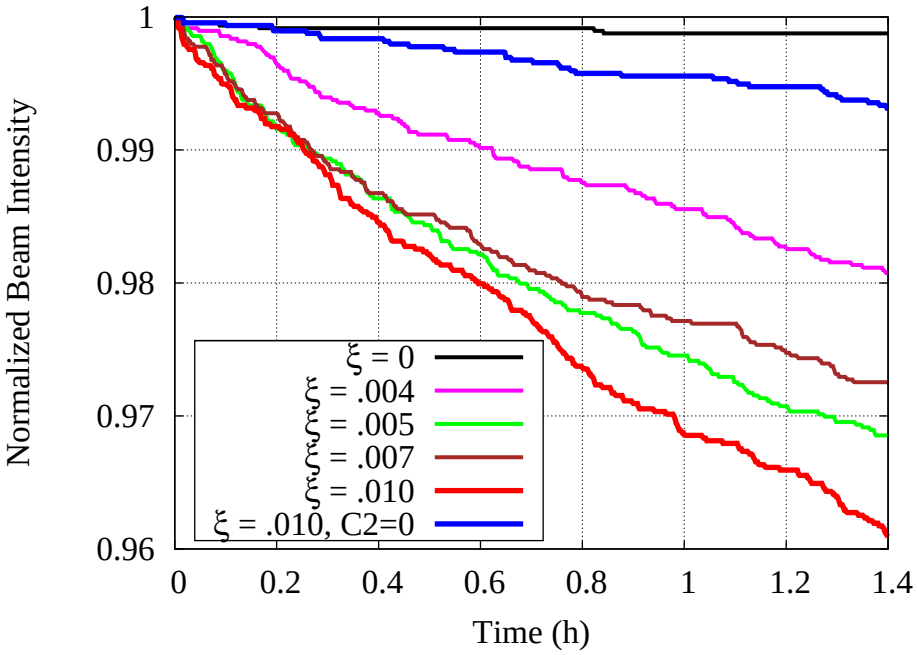

FIG. 12: Proton intensity evolution for different values of beam-beam parameter per IP.

G. Chromaticity

Reducing the betatron tune chromaticity can also be a very powerful instrument in decreasing the particle losses. Results in Fig. 16, demonstrate that changing the tune chromaticity from the present 15-20 units to 5-10 units may significantly improve the beam life time. This can give about 10% in luminosity integral.

H. Further β^* Reduction

An improvement which can be relatively easily implemented is the further reduction of the beta-function at the main IPs. Decreasing the β^* from 35 cm to 28 cm one can gain 10% both in peak luminosity and in luminosity integral.

I. Beams Separation, 23 Bucket Spacing

Since parasitic collisions give a strong contribution to beam-beam effects, the nearest parasitic collision points dominate, one could increase separation of beams in these points thus making their effect weaker. This could be done by changing the bunch filling pattern

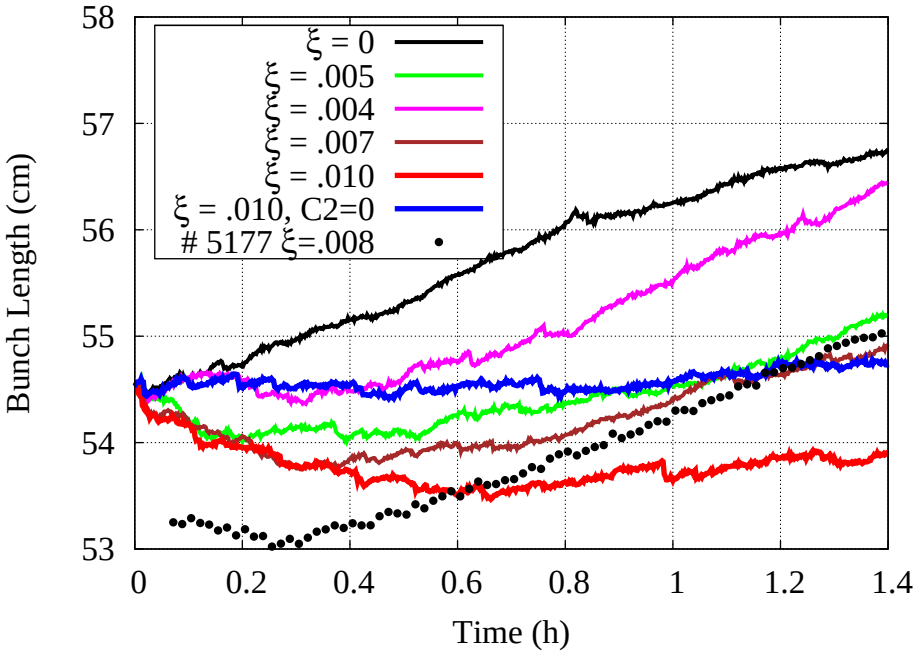

FIG. 13: Effect of corrected second order chromaticity on the proton bunch length evolution.

from 3 trains of 12 bunches with 21 RF buckets between bunches to 3 x 11 bunches with separation of 23 RF buckets, conserving the overall intensity of antiprotons. In that case the separation in the nearest PCs is bumped from 8.2 beam sigmas to 13.6 beam sigmas. Figure 17 shows that such modification allows to increase the attainable beam-beam parameter for antiprotons from 0.01 per IP to 0.0125 without loss in efficiency.

V. NEW COLLISION HELIX

As mentioned, the strong betatron resonances affecting the collider performance are caused by beam-beam effects. It was shown that the strength of the 7-th order resonance is determined by the long range collisions [7]. Also, analytical calculations and numerical simulations predicted that increasing the beam separation at the parasitic collision points nearest to the main IPs would give the largest benefit. To achieve this, two extra electrostatic separators were installed during the 2006 shutdown. As the result of their commissioning, the separation at the IPs upstream and downstream of CDF and D0 increased by 20% (Fig. 18).

The increased separation showed itself in improved proton lifetime. Figure 19 shows

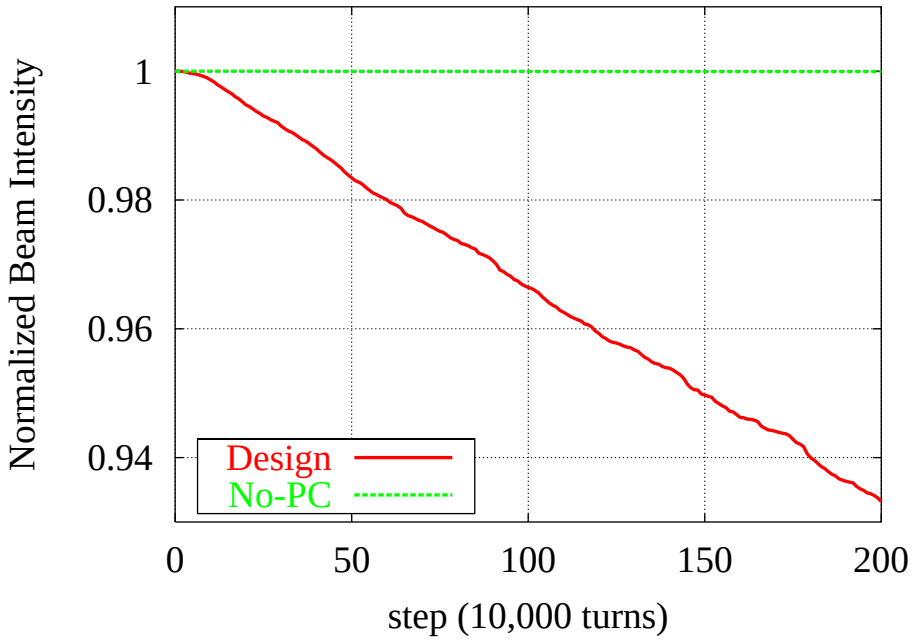

FIG. 14: Normalized intensity of bunch #6 simulated in the presence (solid line) and in the absence (dashed line) of long range collisions.

TABLE II: Radial separations in the first long range collision points in units of the beam size.

	CDF u.s.	**CDF d.s.**	**D0 u.s.**	**D0 d.s.**
Before	5.4	5.6	5.0	5.2
After	6.4	5.8	6.2	5.6

a comparison of the single bunch proton intensity for two HEP stores before and after commissioning of the new helix. Initial intensities and emittances of antiprotons in these stores were close which allows direct comparison.

A noticeable change in the bunch length behavior can be observed in Fig. 20. Note that on the old helix protons experienced significant bunch shortening.

Single bunch luminosity and luminosity integral for the same two stores are shown in Fig. 21. As one can see, luminosity lifetime in the new configuration has improved substantially. The overall gain can be quantified in terms of luminosity integral over a fixed period of time (e.g. 24 hours) normalized by the initial luminosity. The value of this parameter has increased by 16%.

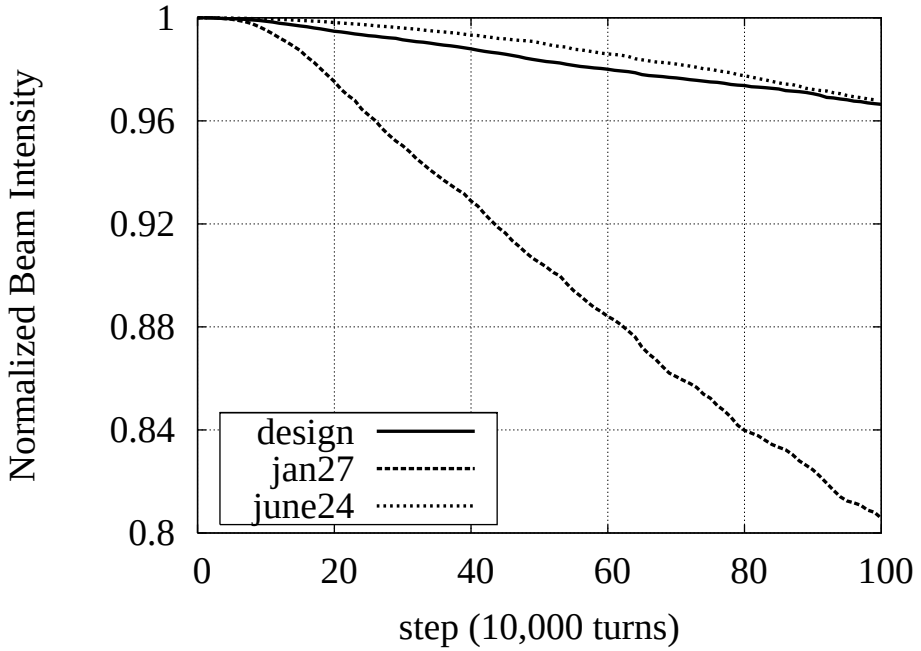

FIG. 15: Intensity of bunch #6 vs. time for different types of optics. $\xi = 0.01$, $Q_x = 0.57$, $Q_Y = 0.56$

VI. SECOND ORDER CHROMATICITY

Increasing the beam separation mitigated the long range beam-beam effects. However, with advances in the antiproton production rate, the initial antiproton intensity at collisions has been rising continuously. Head-on beam-beam parameter for protons was pushed up to 0.008 per IP which made the head-on beam-beam effects in the proton beam much more pronounced. One of the possible ways for improvement is a major change of the betatron tune in order to increase the available tune space. This, however, requires significant investment of the machine time for optics studies and tuning. A partial solution may be implemented by decoupling of the transverse and longitudinal motion at the main IPs, i.e. by reducing the chromatic beta-function.

The value of chromatic beta-function $(\Delta\beta/\beta)/(\Delta p/p)$ at both IPs is -600 which leads to the beta-function change of 10% for a particle with 1σ momentum deviation [9]. Thus, a large variation of focusing for particles in the bunch exists giving rise to beam-beam driven synchrobetatron resonances.

Numerical simulations with weak-strong code predicted that elimination of the chromatic

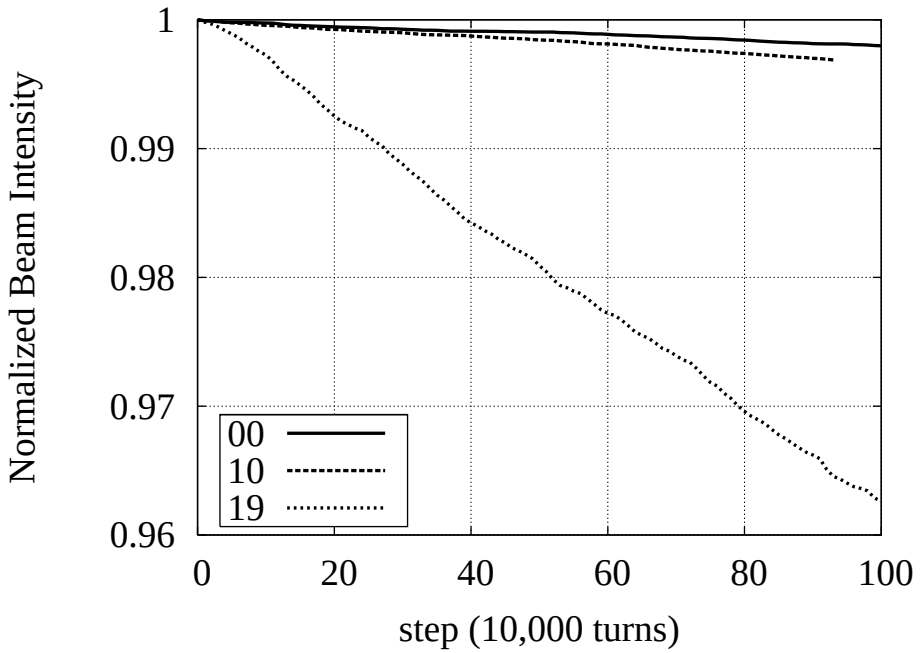

FIG. 16: Evolution of the bunch intensity for various values of betatron tune chromaticity. June optics, $Q_x = 0.58$, $Q_y = 0.575$, $\xi = 0.01$.

beta-function at the main IPs would mitigate the deterioration of proton lifetime at the present values of antiproton intensity even without switching to the new betatron tune working point. In Fig. 22 the simulated proton bunch intensities are plotted for the cases of corrected and uncorrected chromatic beta-function.

In order to achieve the desired smaller beta-function chromaticity, a new scheme of sextupole correctors in the Tevatron has been developed and implemented in May 2007. The scheme uses the existing sextupole magnets split into multiple families instead of just two original SF and SD circuits. The effect of introducing the new circuits is illustrated in Fig. 6.

VII. SUMMARY AND DISCUSSION

Over the past two years Tevatron routinely operated at the values of head-on beam-beam tune shift for both proton and antiproton beams exceeding 0.02. The transverse emittance of antiprotons is a factor of 3 to 5 smaller than the proton emittance. This creates significantly different conditions for the two beams.

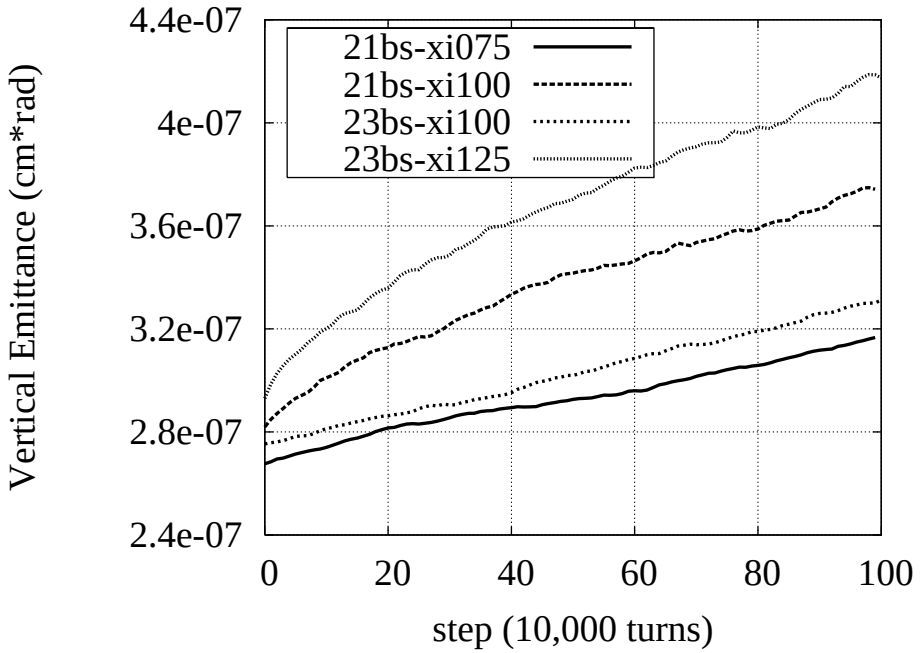

FIG. 17: Vertical emittance of bunch #6 vs. time for the 21 and 23 bucket spacing configurations and different values of beam-beam parameter.

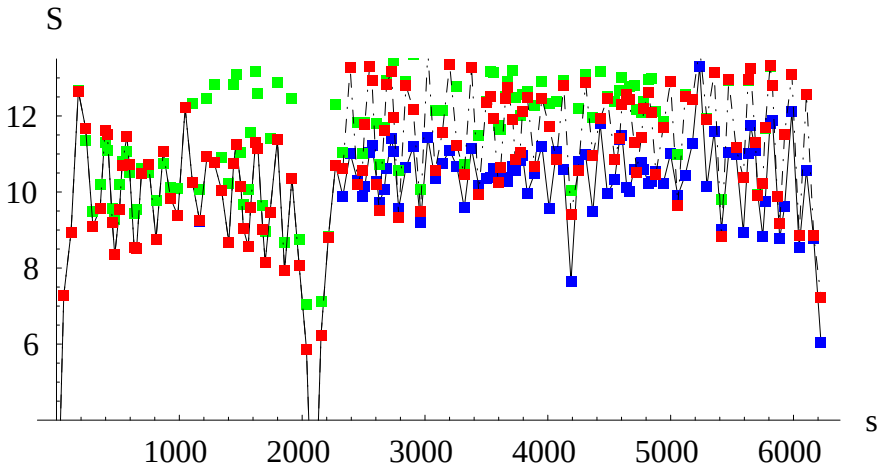

FIG. 18: Radial beam separation at the collision helix in units of the beam size vs. azimuth starting from CDF IP. Blue - design helix, red - before installation of the new separators, green - present.

Beam-beam effects in antiprotons are dominated by long range interactions at four collision points with minimal separation. After the separation at these points was increased to 6σ no adverse effects are observed in antiprotons at present proton intensitites.

On the contrary, protons experience life time degradation due to head-on collisions with

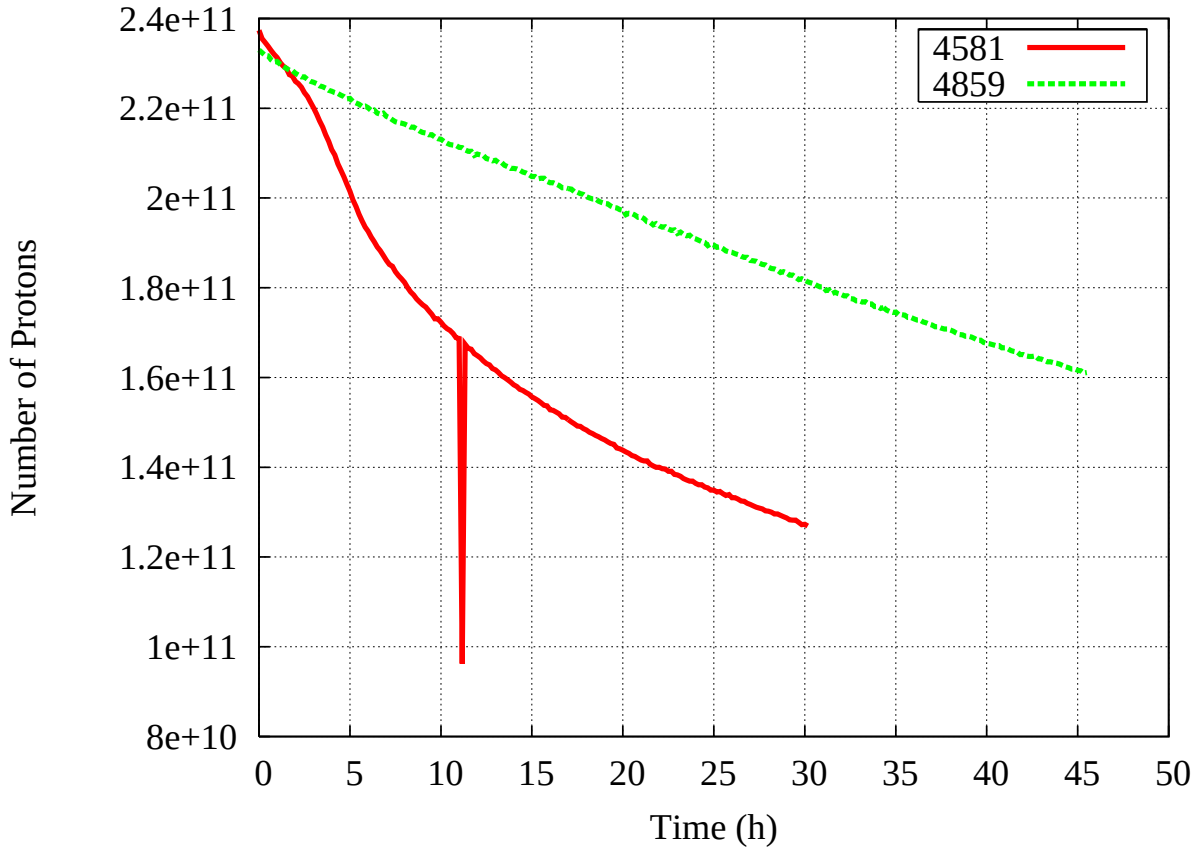

FIG. 19: Single bunch proton intensity in two HEP stores. 4581 with the old helix, 4859 with the new helix.

the beam of smaller transverse size. Correction of chromatic β-function in the final focus and reduction of betatron tune chromaticity increased dynamic aperture and improved proton beam life time.

Simulation of beam-beam effects developed for the Tevatron correctly describes many observed features of the beam dynamics, has predictive power and has been used to support changes of the machine configuration.

Further increase of the beam intensities is limited by the space available on the tune diagram near the current working point. A change of the tune working point from 0.58 to near the half integer resonance would allow as much as 30% increase of intensities but requires a lengthy commissioning period which makes it inlikely that this improvement will be realized during the time remaining in Run II.

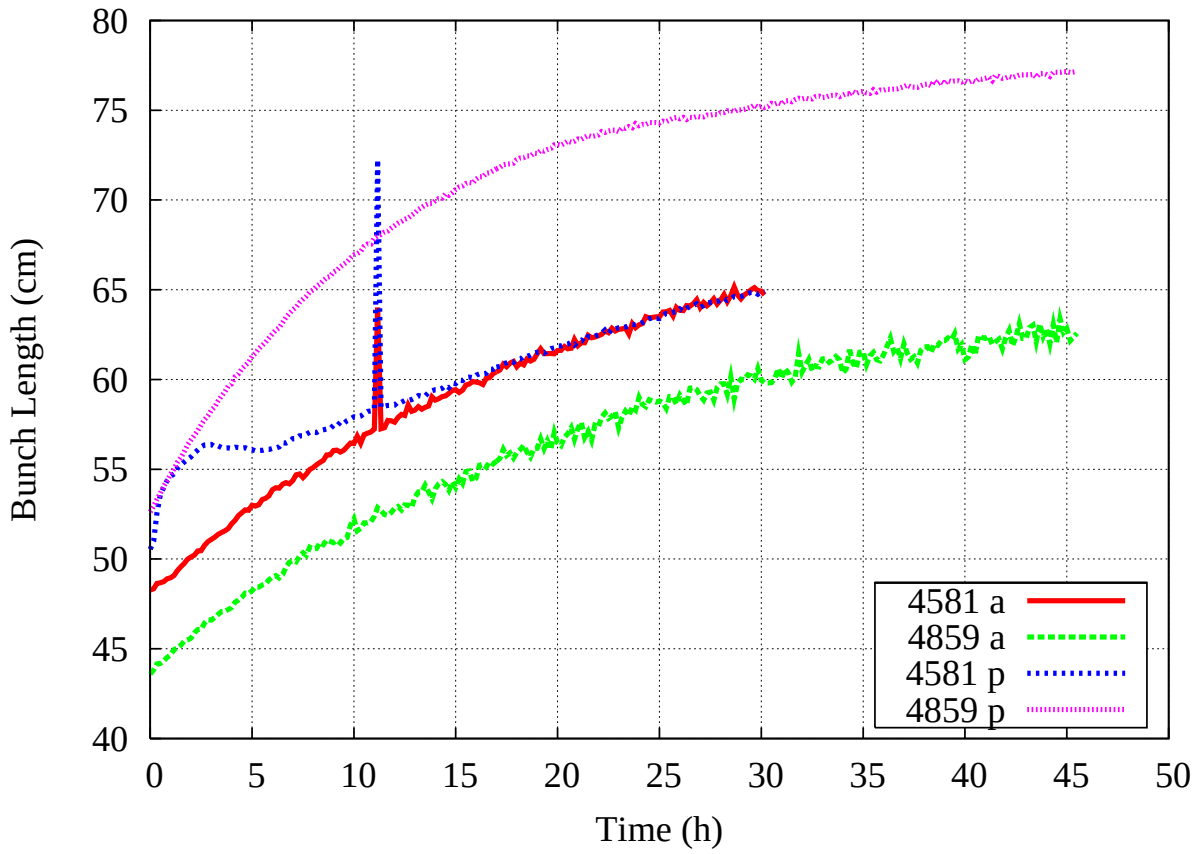

FIG. 20: Proton and antiproton bunch length in two HEP stores. 4581 with the old helix, 4859 with the new helix.

Acknowledgments

This report is the result of hard work and dedication of many people at Fermilab. The work was supported by the Fermi Research Alliance, under contract DE-AC02-76CH03000 with the U.S. Dept. of Energy.

---

[1] V. Shiltsev, Y. Alexahin, V. Lebedev, P. Lebrun, R. S. Moore, T. Sen, A. Tollestrup, A. Valishev, and X. L. Zhang, Phys. Rev. ST Accel. Beams **8**, 101001 (2005).

[2] *Tevatron run ii handbook*, `http://www-bd.fnal.gov/runII`.

[3] P. Ivanov, J. Annala, A. Burov, V. Lebedev, E. Lorman, V. Ranjbar, V. Scarpine, and V. Shiltsev, in *Proceedings of the Particle Accelerator Conference, Portland, OR, USA* (2003), pp. 3062–3064.

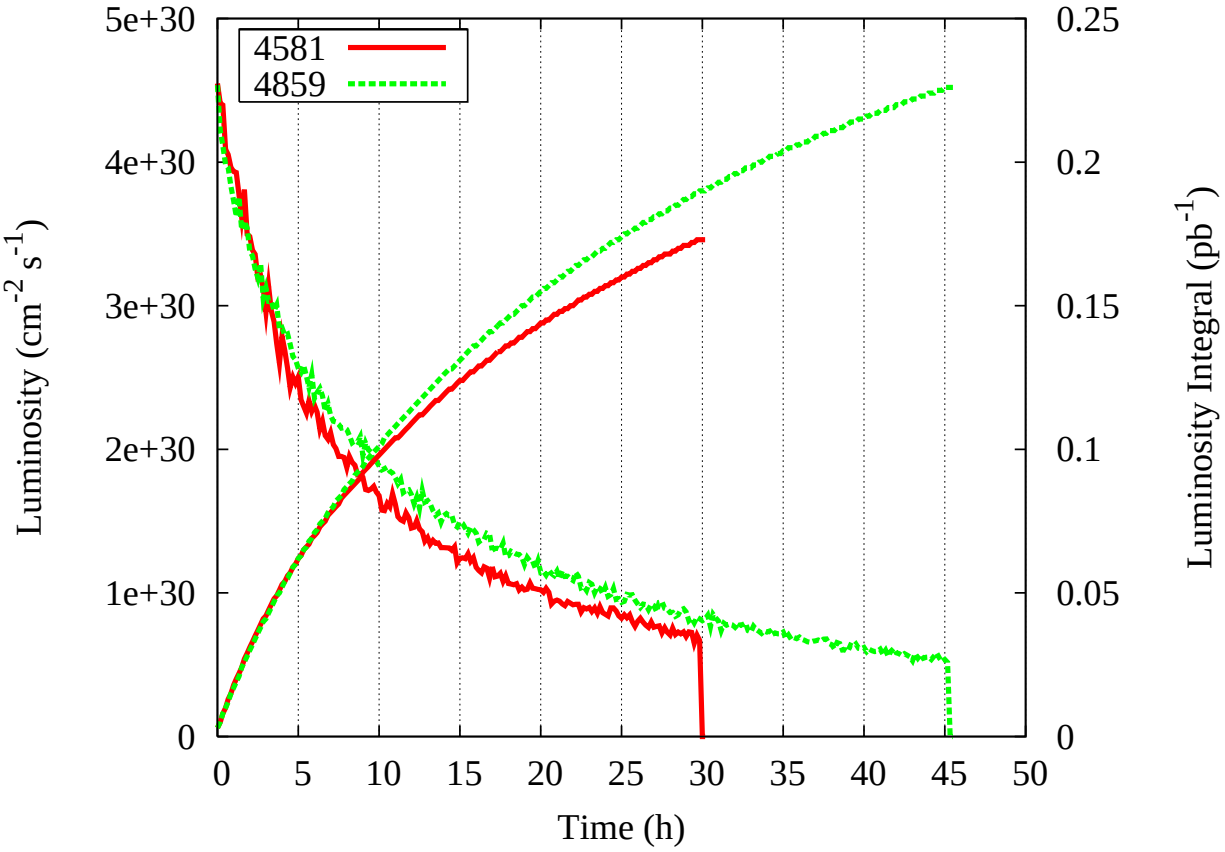

FIG. 21: Single bunch luminosity and luminosity integral for stores 4581 and 4859.

[4] P. Ivanov, Y. Alexahin, J. Annala, V. Lebedev, and V. Shiltsev, in *Proceedings of the Particle Accelerator Conference, Knoxville, TN, USA* (2005), pp. 2714–2716.

[5] V. H. Ranjbar and P. Ivanov, Phys. Rev. ST Accel. Beams **11**, 084401 (2008).

[6] R. Moore, Y. Alexahin, J. Johnstone, and T. Sen, in *Proceedings of the Particle Accelerator Conference, Knoxville, TN, USA* (2005), pp. 1931–1933.

[7] Y. Alexahin, in *Proceedings of the Particle Accelerator Conference, Albuquerque, NM, USA* (2007), pp. 3874–3876.

[8] C.-Y. Tan, to be published.

[9] A. Valishev, G. Annala, V. Lebedev, and R. Moore, in *Proceedings of the Particle Accelerator Conference, Albuquerque, NM, USA* (2007), pp. 3922–3924.

[10] V. Shiltsev and E. McCrory, in *Proceedings of the Particle Accelerator Conference, Knoxville, TN, USA* (2005), pp. 2536–2537.

[11] M. Syphers, *Beam-beam tune distributions with differing beam sizes*, fermilab Beams Doc. 3031.

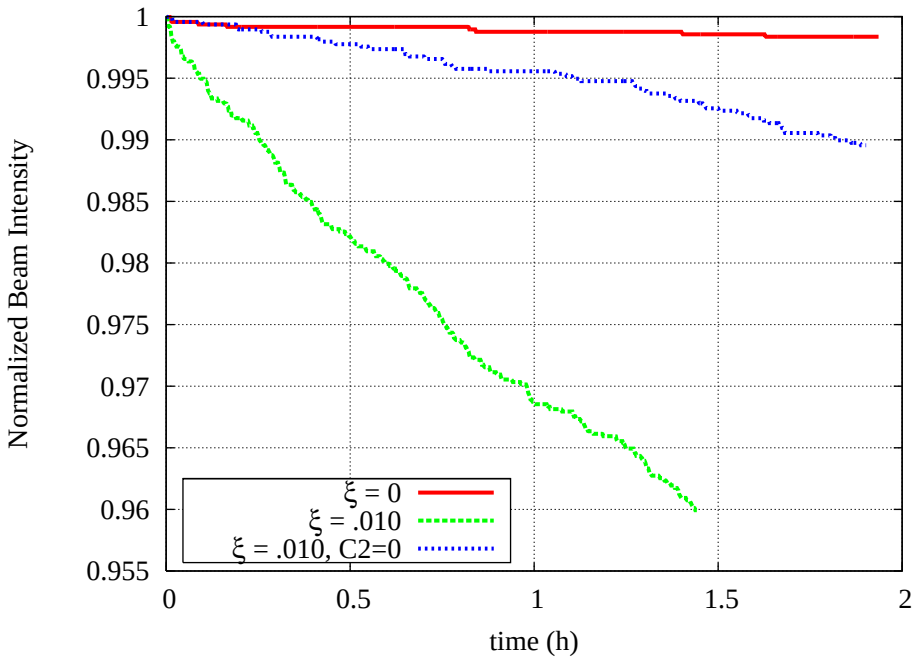

FIG. 22: Normalized intensity of one proton bunch vs. time. Green line - $\xi = 0.01$, chromatic beta-function = -600. Blue line - $\xi = 0.01$, chromatic beta-function = 0. Red line - $\xi = 0$. Numerical simulation.

[12] Y. Alexahin, in *Proceedings of the Particle Accelerator Conference, Knoxville, TN, USA* (2005), pp. 544–548.

[13] V. Lebedev, in *Proceedings of the Particle Accelerator Conference, Portland, OR, USA* (2003), pp. 29–33.

[14] `http://www-bd.fnal.gov/SDAViewersServlets/valishev_sa_catalog2.html`.

[15] D. Shatilov, Part. Accel. **52**, 65 (1996).

[16] K. Hirata, H. Moshammer, and F. Ruggiero (1992), kEK Report 92-117.

[17] V. Sajaev, V. Lebedev, V. Nagaslaev, and A. Valishev, in *Proceedings of the Particle Accelerator Conference, Knoxville, TN, USA* (2005), pp. 3662–3664.

[18] A. Valishev, Y. Alexahin, J. Annala, V. Lebedev, V. Nagaslaev, and V. Sajaev, in *Proceedings of European Accelerator Coference, Edinburgh, Scotland* (2006), pp. 2053–2055.

[19] V. Lebedev, V. Nagaslaev, A. Valishev, and V. Sajaev, Nucl. Instrum. Methods Phys. Res., Sect. A **558**, 299 (2006).

[20] V. Lebedev, `http://www-bdnew.fnal.gov/pbar/organizationalchart/lebedev/OptiM/optim.htm`.

[21] V. Lebedev and S. Bogacz, `http://www.cebaf.gov/~lebedev/AccPhys/`.

[22] V. Lebedev and A. Burov, in *Proceedings of the 33rd ICFA Advanced Beam Dynamics Workshop on High Intensity and High Brightness Hadron Beams, ICFA-HB2004, Bensheim, Germany* (2004), pp. 350–354.